"Physics of Semiconductor Devices" S.M.Sze

Diody LED i lasery półprzewodnikowe.

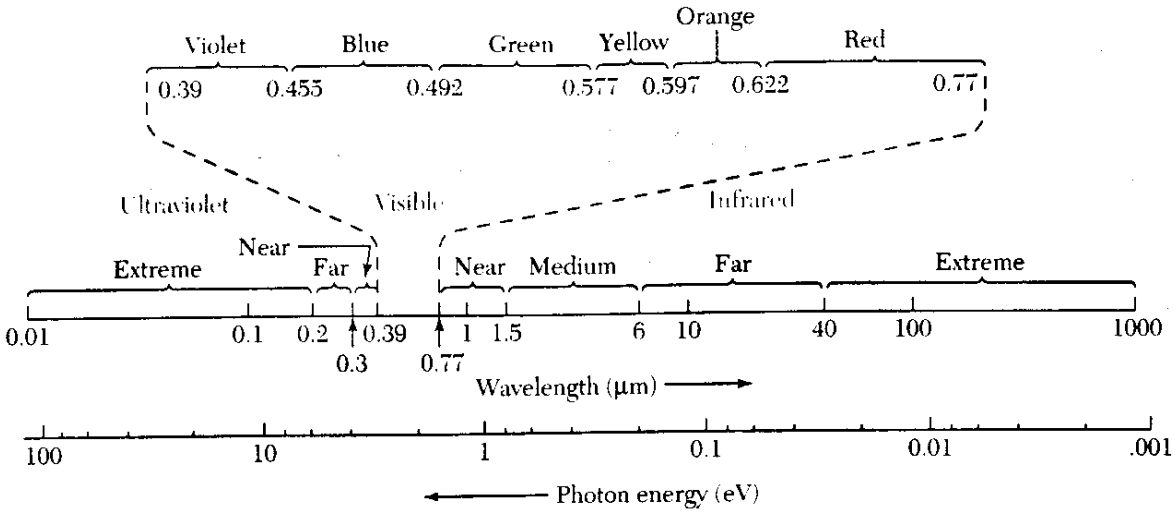

Fig. 1 Chart of the electromagnetic spectrum from the ultraviolet region to the infrared region.

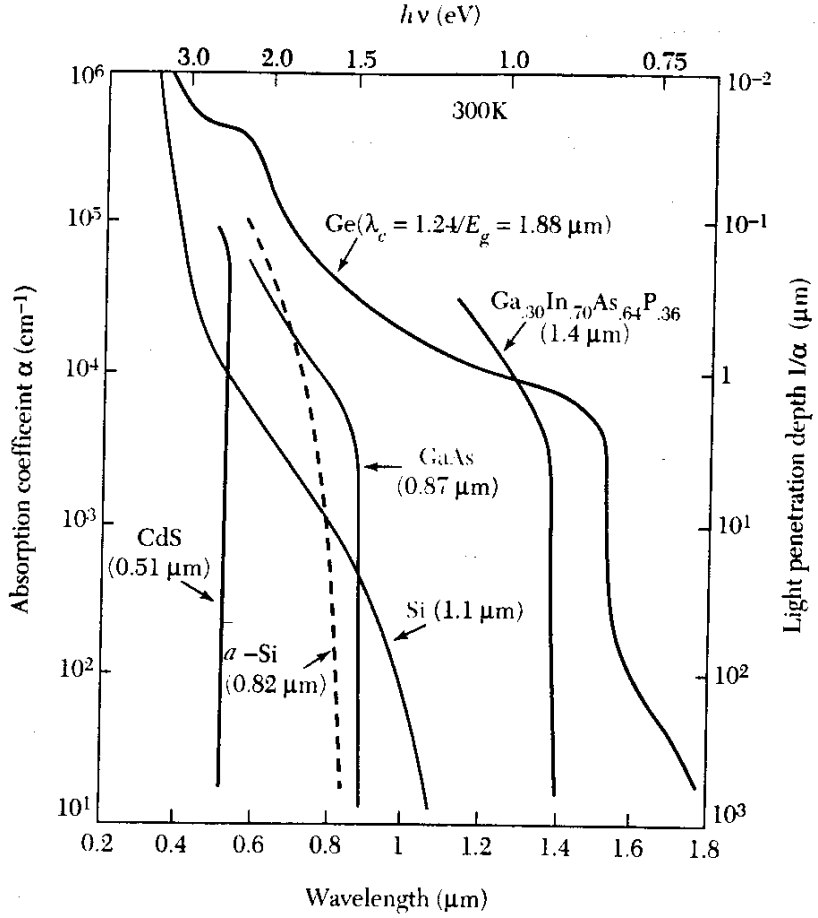

Fig. 5 Optical absorption coefficients for various semiconductor materials.[2] The value in the parenthesis is the cutoff wavelength.

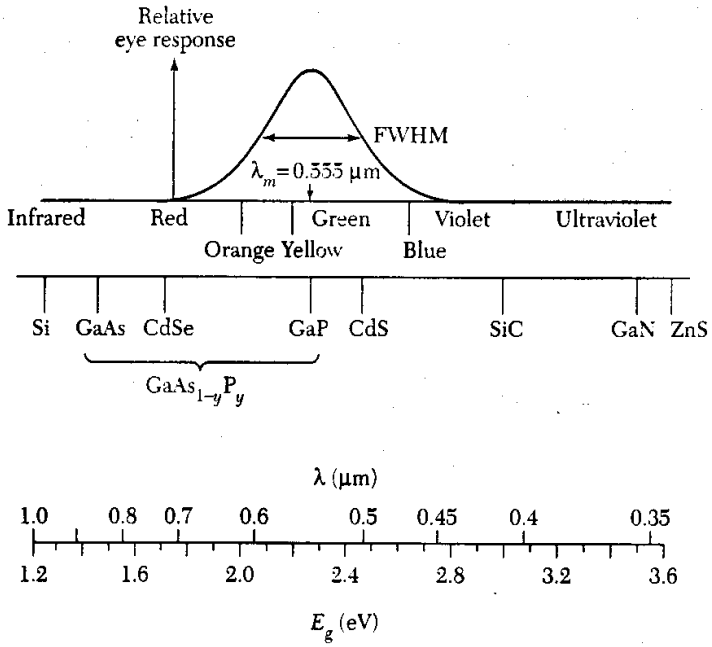

Fig. 6 Semiconductors of interest as visible LEDs. Figure includes relative response of the human eye.

TABLE 1 Common III-V materials used to produce LEDs and their emission wavelengths.

Material	Wavelength (nm)
InAsSbP/InAs	4200
InAs	3800
GaInAsP/GaSb	2000
GaSb	1800
$Ga_xIn_{1-x}As_{1-y}P_y$	1100-1600
$Ga_{0.47}In_{0.53}As$	1550
$Ga_{0.27}In_{0.73}As_{0.63}P_{0.37}$	1300
GaAs:Er,InP:Er	1540
Si:C	1300
GaAs:Yb,InP:Yb	1000
$Al_xGa_{1-x}As$:Si	650-940
GaAs:Si	940
$Al_{0.11}Ga_{0.89}As$:Si	830
$Al_{0.4}Ga_{0.6}As$:Si	650
$GaAs_{0.6}P_{0.4}$	660
$GaAs_{0.4}P_{0.6}$	620
$GaAs_{0.15}P_{0.85}$	590
$(Al_xGa_{1-x})_{0.5}In_{0.5}P$	655
GaP	690
GaP:N	550-570
$Ga_xIn_{1-x}N$	340,430,590
SiC	400-460
BN	260,310,490

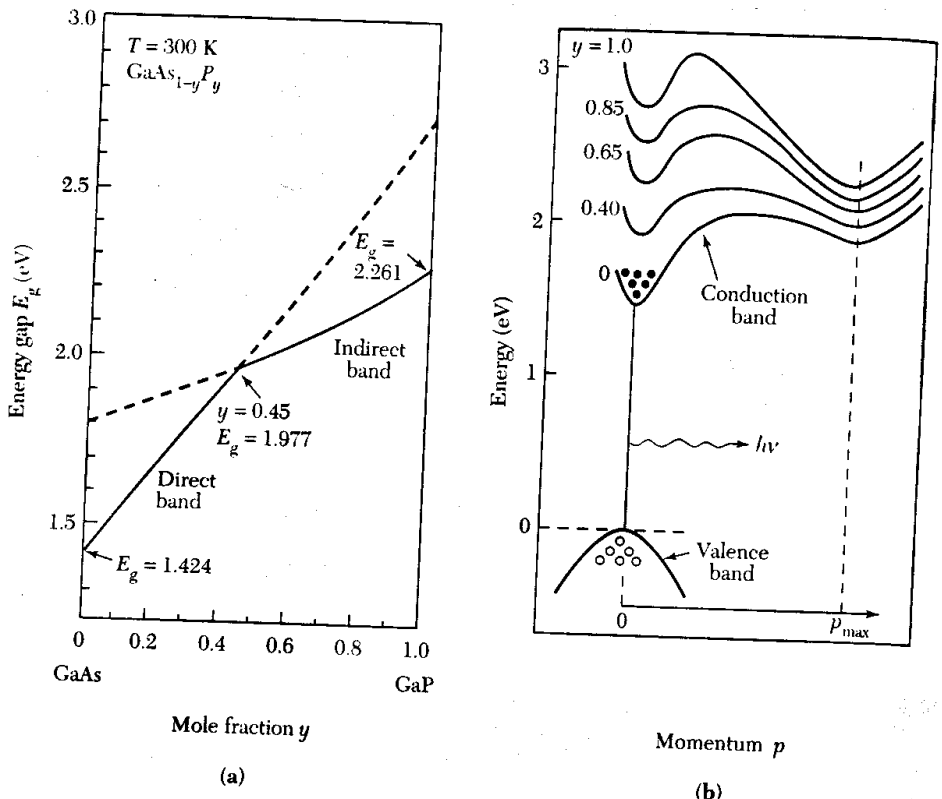

Fig. 7 (a) Compositional dependence for the direct- and indirect-energy bandgap for $GaAs_{1-y}P_y$. (b) The alloy compositions shown correspond to red (y = 0.4), orange (0.65), yellow (0.85), and green light (1.0). [3]

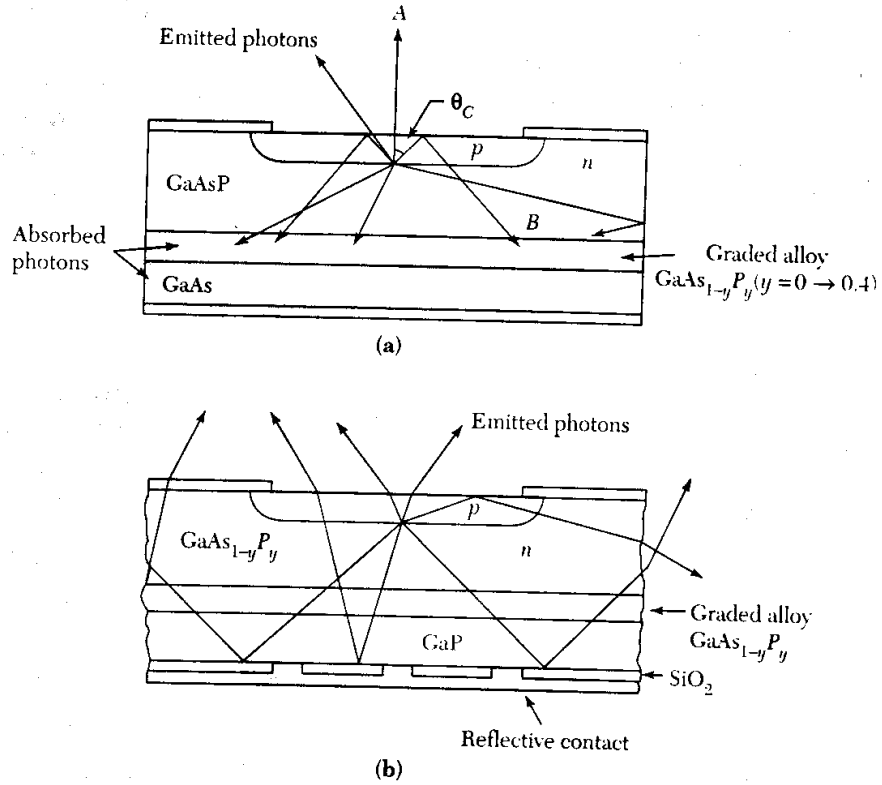

Fig. 9 Basic structure of a flat-diode LED and the effects of (*a*) an opaque substrate ($GaAs_{1-y}P_y$) and (*b*) a transparent substrate (GaP) on photons emitted at the *p-n* junction. [5]

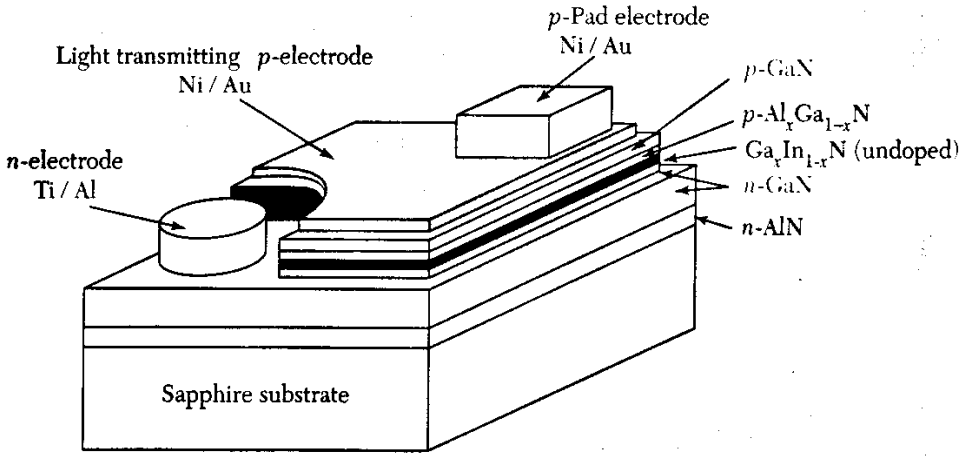

Fig. 10 III-V nitride LED grown on sapphire substrate.[6]

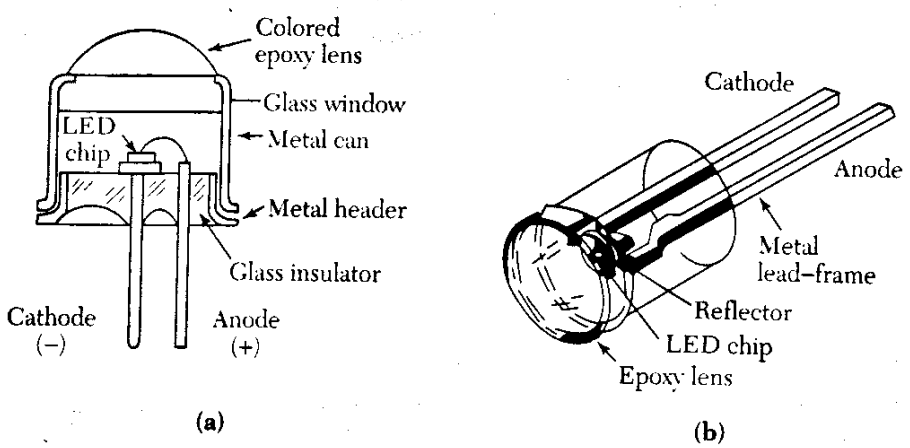

Fig. 11 Diagrams of two LED lamps.[8]

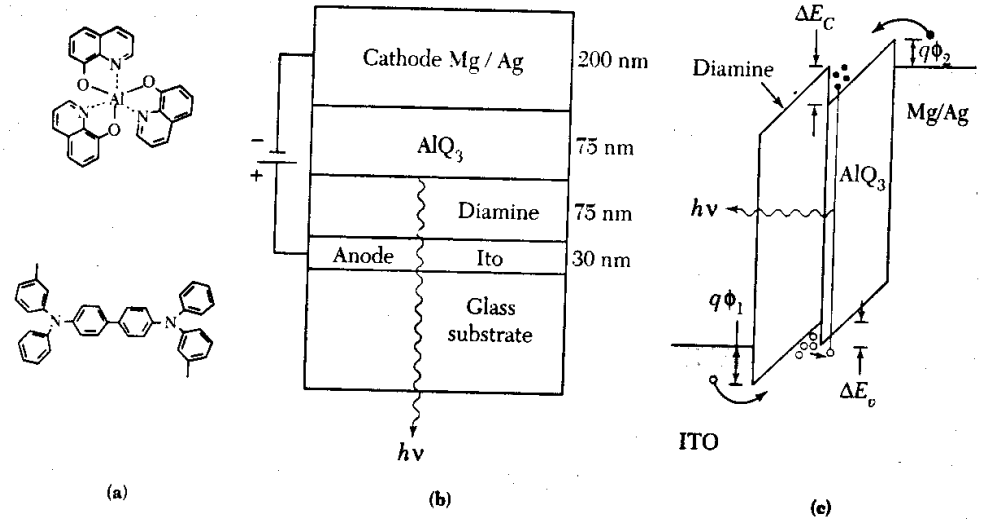

Fig. 13 (*a*) Organic semiconductors. (*b*) OLED cross sectional view. (*c*) Band diagram of an OLED.

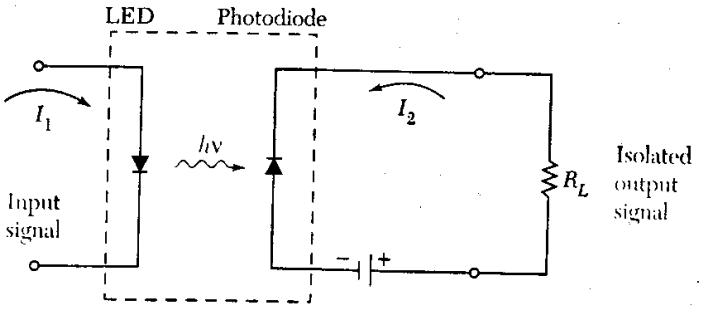

Fig. 14 An opto-isolator in which an input signal is decoupled from the output signal.

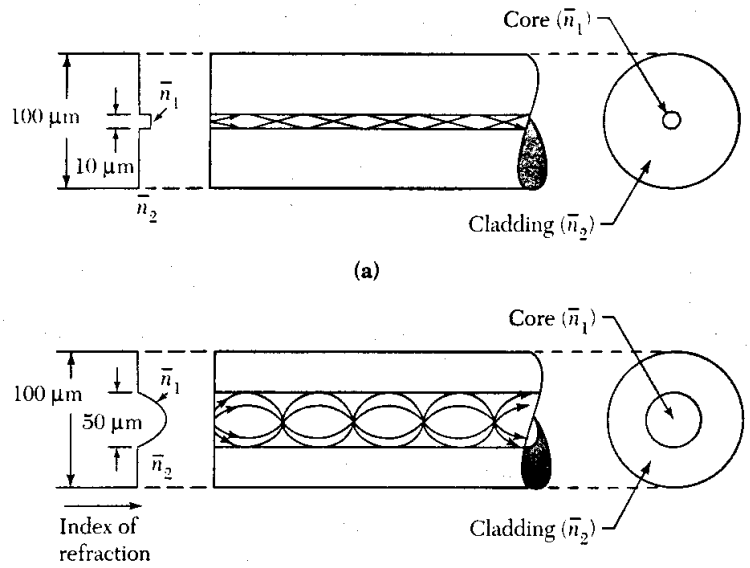

Fig. 15 Optical fibers. (*a*) Step-index fiber having a core with slightly larger reflective index. (*b*) Graded-index fiber having a parabolic grading of the reflective index in the core.[11]

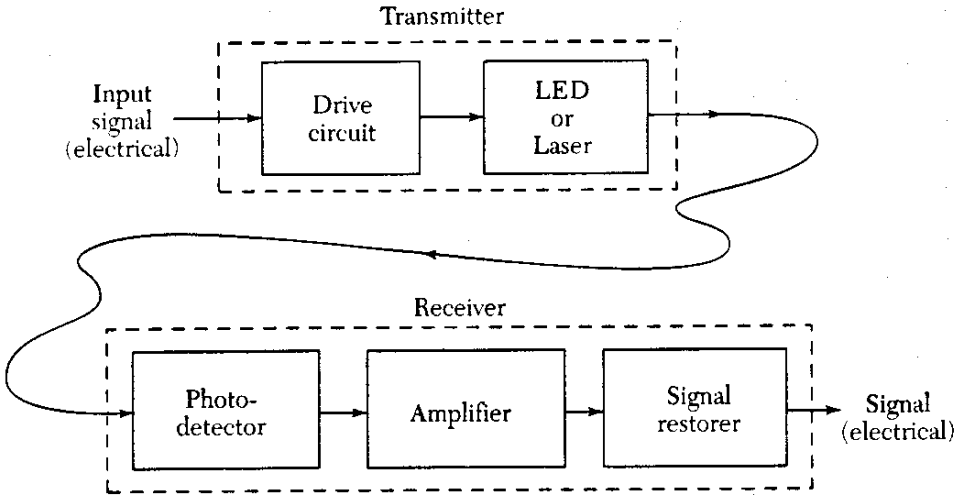

Fig. 16 Basic elements of an optical fiber transmission link.

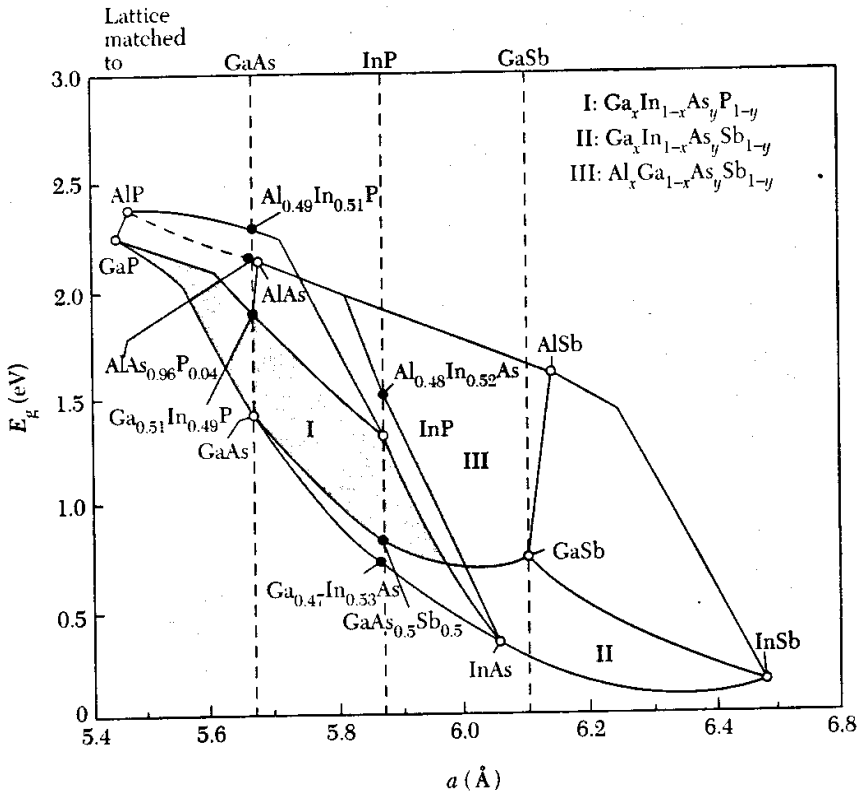

Fig. 18 Energy bandgap and lattice constant for three III-V compound solid alloy system. [13]

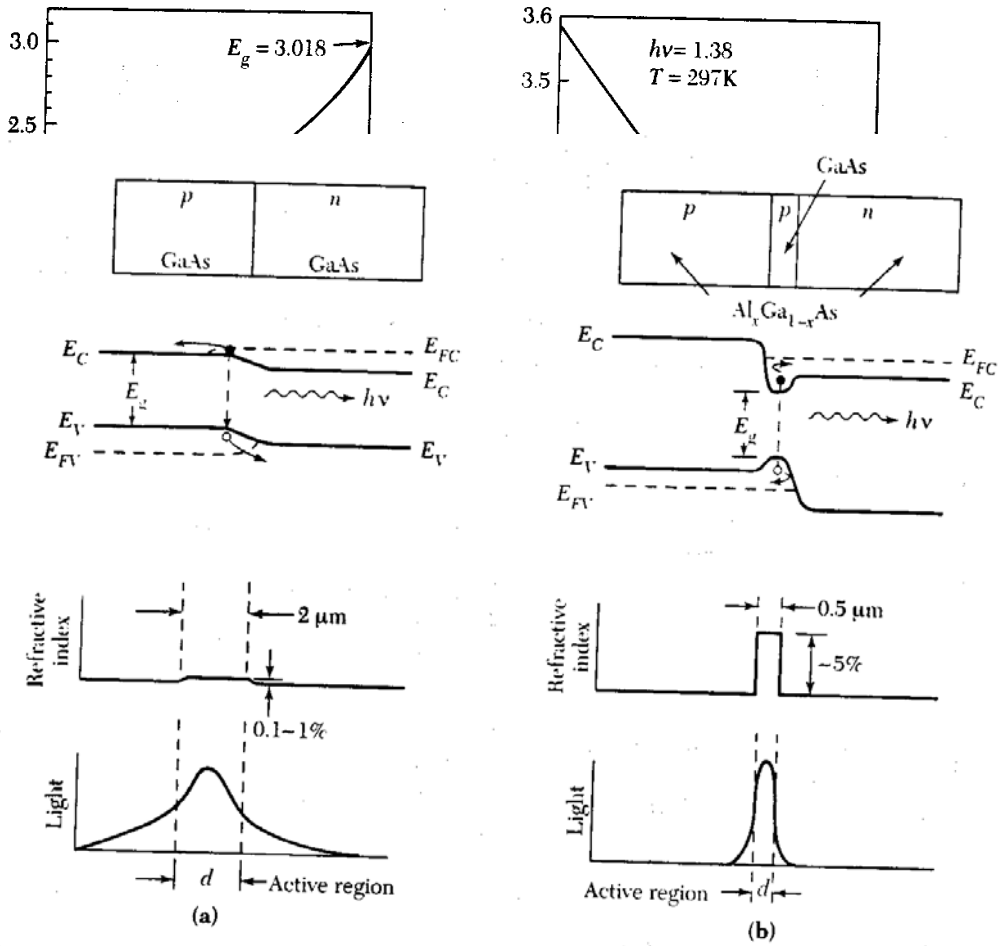

Fig. 1 denc

Fig. 20 Comparison of some characteristics of (*a*) homojunction laser and (*b*) double-heterojunction (DH) laser. Second from the top row shows energy band diagrams under forward bias. The refractive index change for a homojunction laser is less than 1%. The refractive index change for DH laser is about 5%. The confinement of light is shown in the bottom row. [14]

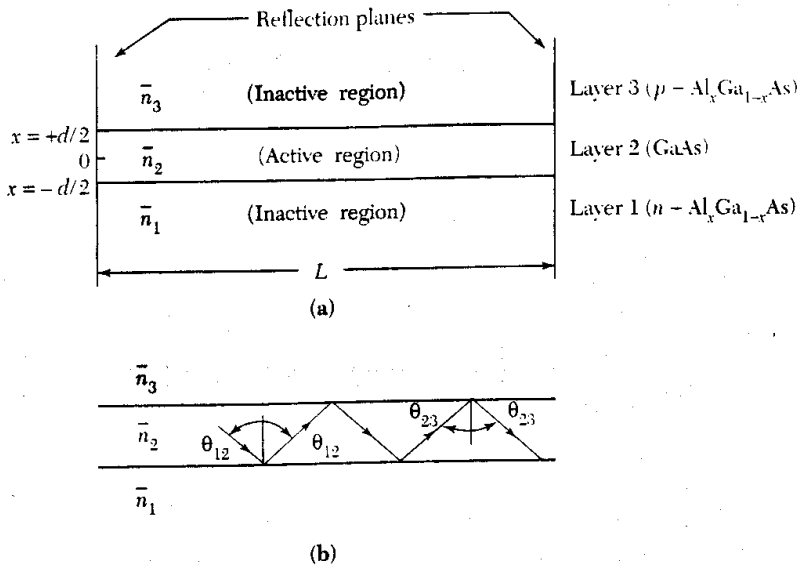

Fig. 21 (*a*) Representation of a three-layer dielectric waveguide. (*b*) Ray trajectories of the guided wave.

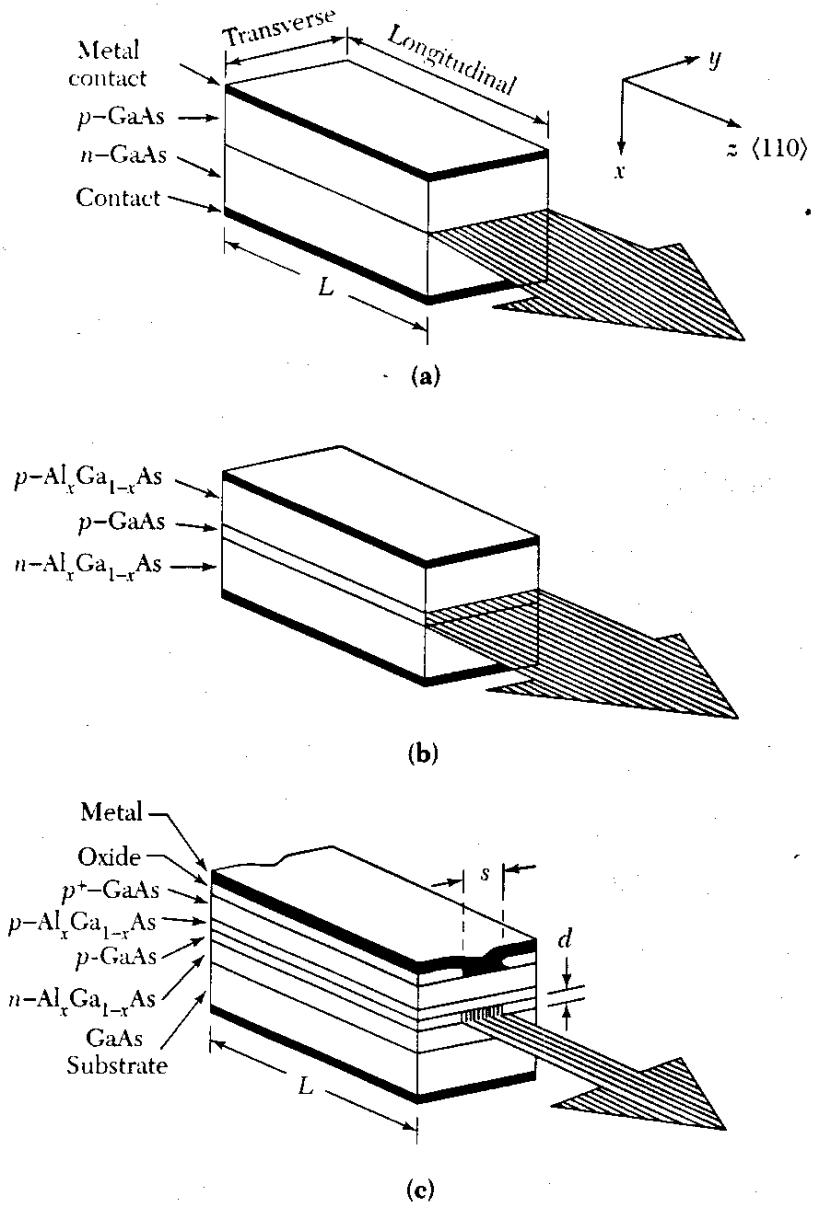

Fig. 23 Semiconductor laser structure in the Fabry–Perot-cavity configuration. (*a*) Homojunction laser. (*b*) Double-heterojunction (DH) laser. (*c*) Stripe-geometry DH laser. [14,15]

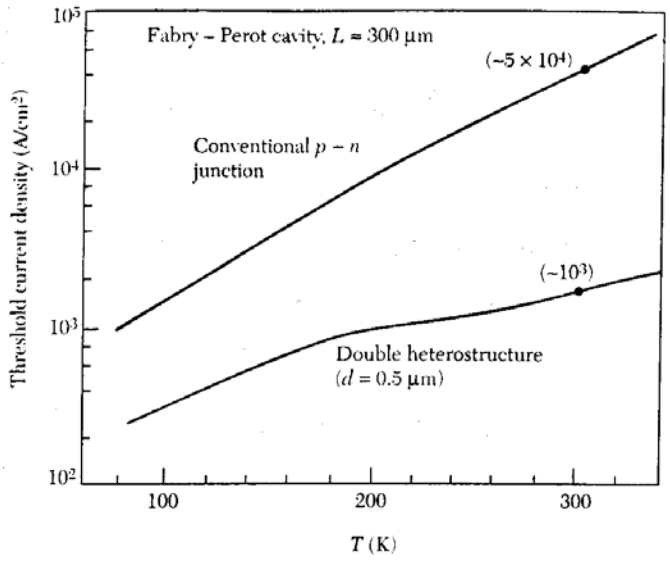

Fig. 24 Threshold current density versus temperature for the two laser structures shown[14] in Fig. 20.

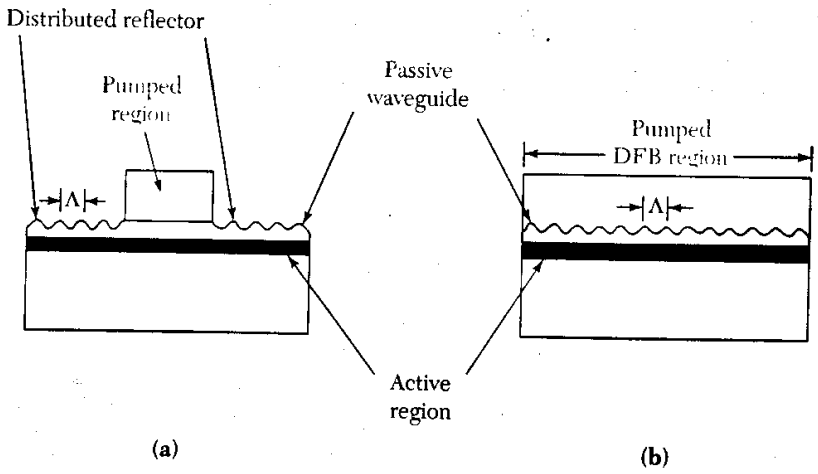

Fig. 27 Two methods of obtaining a single-frequency laser. (*a*) Distributed Bragg reflector (DBR) laser, and (*b*) a distributed feedback (DFB) laser.

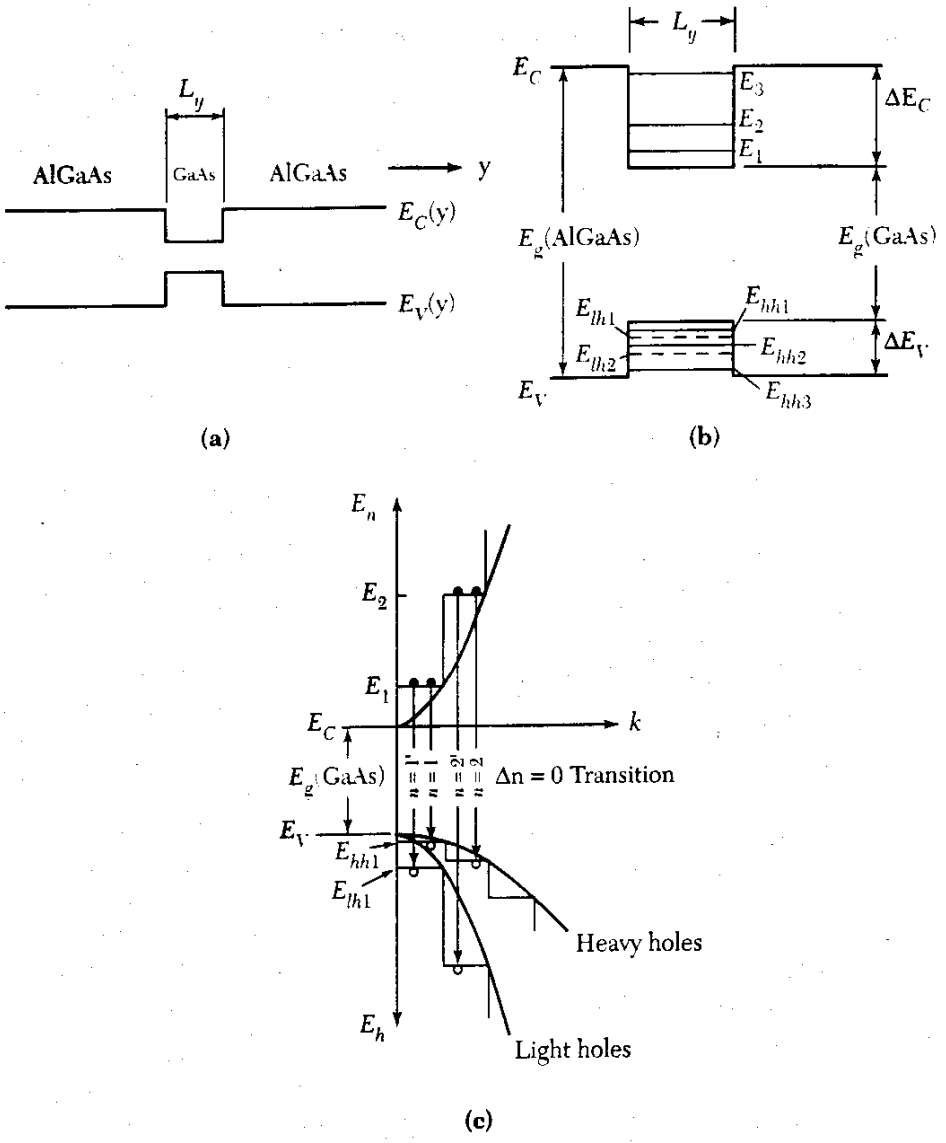

Fig. 28 The quantum-well (QW) laser: (*a*) single GaAs QW surrounded by AlGaAs, (*b*) discrete energy levels within the well, and (*c*) density of states for electrons and holes within the well.

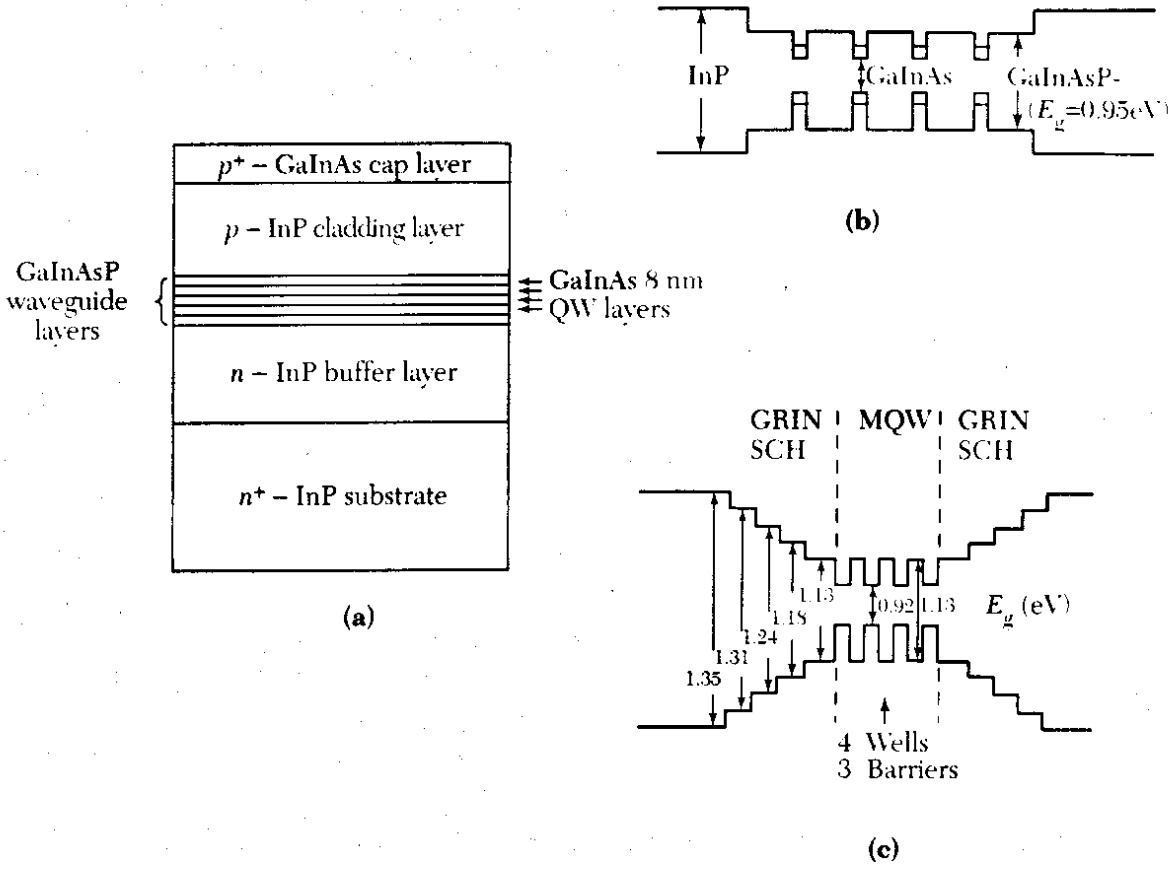

Fig. 29 (*a*) Schematic of the cross section of an GaInAs/GaInAsP multiple-quantum-well laser structure. (*b*) Schematic of the bandgaps of the SCH-MQW layers shown in (*a*). (*c*) GRIN-SCH-MQW structure with thin layers of increasing bandgaps to approximate the graded-index change. [20]